

## Incommensurate modulation in the high- $T_c$ superconductor $\text{Ba}_{1-x}\text{K}_x\text{BiO}_3$ and its relation to the conducting properties

M. Verwerft and G. Van Tendeloo

*University of Antwerp (R.U.C.A.), Groenenborgerlaan, 171, B-2020 Antwerp, Belgium*

D. G. Hinks, B. Dabrowski, D. R. Richards, A. W. Mitchell, D. T. Marx, Shiyong Pei, and J. D. Jorgensen

*Materials Science Division, Argonne National Laboratory, Argonne, Illinois 60439*

(Received 16 January 1991; revised manuscript received 10 April 1991)

The incommensurate modulation in  $\text{Ba}_{1-x}\text{K}_x\text{BiO}_3$  is studied by means of electron diffraction. Attention is paid to the symmetry of the modulation and the effect of electron irradiation. Interpretation of the modulation symmetry in cubic samples ( $0.3 < x < 0.5$ ) as well as in orthorhombic samples ( $0.1 < x < 0.3$ ) in the framework of a four-dimensional description allows one to determine it as a periodic displacement of the bismuth atoms. Satellite reflections corresponding to the modulation are observed only after irradiation with electrons. However, since the critical voltage is below 40 kV, it is believed that the modulation is in fact a fundamental material property. The incommensurability of the modulation for  $x < 0.4$  results in a partial charge disproportionation on the bismuth sites, which can explain the lack of superconducting properties for  $\text{Ba}_{1-x}\text{K}_x\text{BiO}_3$  with  $x < 0.4$ . In the superconducting phase  $\text{Ba}_{0.6}\text{K}_{0.4}\text{BiO}_3$ , the modulation is commensurate, and high-resolution observations provide evidence for a modulation model without charge disproportionation, yielding a metallic behavior at room temperature.

### I. INTRODUCTION

It is well known that the discovery of high- $T_c$  superconductivity in the La-Ba-Cu-O system by Bednorz and Müller<sup>1</sup> was at least partially inspired by their knowledge of the superconducting properties of the  $\text{BaPb}_{1-x}\text{Bi}_x\text{O}_3$  perovskite system. Superconductivity in  $\text{BaPb}_{1-x}\text{Bi}_x\text{O}_3$  with a transition temperature of  $\approx 12$  K had been reported by Sleight, Gillson, and Bierstedt.<sup>2</sup>

The worldwide search for high- $T_c$  ceramic materials, which started after the discovery of Bednorz and Müller, was focused in the beginning on Cu-containing compounds. This research has resulted in the discovery of superconductivity in the Y-Ba-Cu-O, Bi-Sr-Cu-O, Tl-Ba-Ca-Cu-O, etc., systems. All these materials contain two-dimensional (2D) copper oxide layers, and it is generally assumed that the superconductivity is related to the mixed valence of copper in these ceramics. From theoretical point of view, it would be very exciting if the phenomenon of high- $T_c$  superconductivity would also occur in materials without such 2D copper oxide layers. This idea put new interest in the research of the "old" systems of oxide superconductors based on  $\text{BaBiO}_3$  and resulted in the discovery of superconducting properties in potassium-substituted  $(\text{Ba,K})\text{BiO}_3$ .<sup>3</sup> At the composition  $\text{Ba}_{0.6}\text{K}_{0.4}\text{BiO}_3$ , this system shows bulk superconductivity with a transition temperature of  $\approx 30$  K,<sup>4</sup> which is well above the transition temperature of conventional superconductors and is surpassed only by that of copper-containing ceramic materials.

The basic structure of  $\text{Ba}_{1-x}\text{K}_x\text{BiO}_3$  is that of the perovskite  $\text{ABO}_3$  ( $A = \text{Ba}$  or  $\text{K}$ ,  $B = \text{Bi}$ ), with the potassium atoms randomly distributed over the Ba sites. It

consists of a framework of corner-linked oxygen octahedra. The center of each octahedron is occupied by a B-type atom (Bi) and the sites in between the octahedra by an A-type atom (Ba or K). Ideally, it has cubic  $Pm\bar{3}m$  symmetry (with unit-cell parameter  $a_p$ ), but depending on composition and temperature, the rigid tilt of the  $\text{BO}_6$  octahedra, combined with the deformation of the octahedra themselves ("breathing-mode distortion"), gives rise to a number of structural phase transitions. The phase diagram as function of both potassium content and temperature has been determined by neutron-diffraction methods.<sup>5</sup>

The crystal structure of nonsubstituted  $\text{BaBiO}_3$  has been investigated by neutron- and x-ray-diffraction methods.<sup>5-10</sup> Its room-temperature structure is derived from the ideal perovskite structure by rigid tilting of the oxygen octahedra about the  $[110]_p$  cubic direction: ( $a^-a^-c^0$ ) tilt in Glazer's notation,<sup>11</sup> combined with deformation of the octahedra (breathing-mode distortion). If only the rigid tilt of the oxygen octahedra were present, the space group would be  $Ibmm$ , based on a  $\sqrt{2}a_p \times \sqrt{2}a_p \times 2a_p$  unit cell, and the four bismuth sites in each unit cell would be equivalent. The breathing-mode distortion of the octahedra lifts this equivalency of the bismuth sites. The resulting monoclinic structure is based on a unit cell with parameters  $a_m \approx b_m \approx \sqrt{2}a_p$ ,  $c_m = 2a_p$ , and  $\beta_m \approx 90^\circ$  with space group  $I2/m$ . The monoclinic unit cell contains two crystallographically inequivalent bismuth sites. The average Bi-O distance for the two inequivalent sites in  $\text{BaBiO}_3$  being significantly different, Cox and Sleight<sup>6</sup> and Thorton and Jacobsen<sup>8</sup> concluded that the bismuth cations are disproportionated in  $\text{Bi}^{3+}$  and  $\text{Bi}^{5+}$ . Subsequent studies by

Mattheiss and Hamann<sup>12</sup> and Chaillout *et al.*<sup>9</sup> did not confirm these results: They concluded that the charge transfer is only minimal and that either the effective valence state is close to 4+ (Mattheiss and Hamann) or that the  $\text{Bi}^{3+}$  and  $\text{Bi}^{5+}$  cations are randomly distributed over the two independent sites (Chaillout *et al.*). More recently, Chaillout *et al.*<sup>10</sup> showed that, depending on the specimen preparation, the  $\text{Bi}^{3+}$ - $\text{Bi}^{5+}$  cations are either randomly distributed over the two independent Bi sites or partially ordered, which reconciles all previous reports on the Bi valence in  $\text{BaBiO}_3$ .

According to electron-band calculations performed by Mattheiss and Hamann,<sup>12</sup> nondistorted  $\text{BaBiO}_3$  should show metallic behavior, which is clearly not the case.<sup>13</sup> Taking into account the structural distortions, their calculations show an energy-band splitting near the Fermi energy level, which explains the observed semiconducting properties of pure  $\text{BaBiO}_3$ . The cubic-to-monoclinic structural distortion consists of two components, as is discussed above: (a) a rigid rotation of  $\text{BiO}_6$  octahedra ( $a^-a^-c^0$  tilt) and (b) a breathing-mode distortion that creates two distinct Bi sites with different average Bi-O distances and, thus, charge disproportionation. Making use of tight-binding arguments, Mattheiss and Hamann conclude that the creation of the energy gap at the Fermi surface (and therefore also the semiconducting behavior) is due to the breathing-mode distortion.

It is observed from the phase diagram of Fig. 1 that as barium is partly substituted by potassium, the breathing-mode distortion is rapidly suppressed and the material transforms from a monoclinic  $I2/m$  to an orthorhombic  $Ibmm$  structure. In this phase the rigid tilt of the octahedra remains ( $a^-a^-c^0$ ). Only one crystallographically inequivalent bismuth site is present in this structure. Electrical resistivity measurements clearly show that orthorhombic  $\text{Ba}_{1-x}\text{K}_x\text{BiO}_3$  is semiconducting also in this composition range.<sup>14,15</sup> This is surprising since it was concluded that the semiconducting properties of  $\text{BaBiO}_3$

are related to the breathing-mode distortion.<sup>12</sup>

Further substitution of barium by potassium eventually suppresses the rigid tilt of the  $\text{BiO}_6$  octahedra, and a primitive cubic phase is formed. The structure of this phase is the ideal perovskite structure with  $Pm\bar{3}m$  symmetry. This cubic phase persists on further substitution of potassium up to the solubility limit. Superconductivity occurs only in the cubic material, i.e., for  $x \geq 0.37$ , and disappears on crossing a metal-to-semiconductor phase boundary on lowering the potassium content.<sup>14-16</sup>

The behavior of  $\text{Ba}_{1-x}\text{K}_x\text{BiO}_3$  is very similar to that of  $\text{BaPb}_{1-x}\text{Bi}_x\text{O}_3$ , which also shows superconducting behavior near a metal-to-insulator transition which is accompanied by a structural phase transition.<sup>2</sup>  $\text{BaPb}_{1-x}\text{Bi}_x\text{O}_3$  has been studied theoretically as well as experimentally in the past 15 years. A major part of the studies are concerned with the semiconducting behavior of the  $\text{BaPb}_{1-x}\text{Bi}_x\text{O}_3$  system in the composition range  $0.35 < x < 1$ . The suggestions that have been proposed to account for the semiconductivity of the heavily doped  $\text{BaPb}_{1-x}\text{Bi}_x\text{O}_3$  system are equally well cited in order to explain the semiconducting behavior in the  $\text{Ba}_{1-x}\text{K}_x\text{BiO}_3$  system for  $0 < x < 0.37$ .<sup>5</sup> In this respect different models have been proposed in the literature: the semiconducting behavior is attributed to either phase separation,<sup>12,17</sup> a "local charge-density wave,"<sup>18,19</sup> a chemical ordering wave,<sup>20</sup> or a long-range incommensurate charge-density wave.<sup>21</sup> Since the postulated structural features that are invoked in these theories either have not been established experimentally (for the local charge-density wave and the chemical ordering wave picture) or are subject to fundamental disagreement among different work groups about their nature or relevance (for the incommensurate charge-density wave and the phase-separation model, respectively), the semiconducting behavior in the  $\text{BaPb}_{1-x}\text{Bi}_x\text{O}_3$  and  $\text{Ba}_{1-x}\text{K}_x\text{BiO}_3$  systems is still an intriguing problem. In this paper we will add some experimental information based on electron-diffraction and high-resolution microscopy observations. This will shed some new light on old controversies.

## II. INCOMMENSURATE MODULATION IN $\text{Ba}_{1-x}\text{K}_x\text{BiO}_3$

A structural modulation which is incommensurate with the basic lattice was first reported by Chaillout and Remeika<sup>22</sup> in an x-ray and electron-diffraction study on oxygen-deficient  $\text{BaBiO}_{3-\delta}$ . Pei *et al.*<sup>5,23</sup> observed a modulation in potassium-substituted  $\text{Ba}_{1-x}\text{K}_x\text{BiO}_3$  (with stoichiometric oxygen content) for all of the nonsuperconducting samples in an electron-diffraction study. They showed that the modulation wavelength varies systematically with the potassium content. For nonsubstituted  $\text{BaBiO}_3$  their value for the modulation wavelength is equal to that reported previously by Chaillout and Remeika for oxygen-deficient  $\text{BaBiO}_{3-\delta}$ . Hewat *et al.*<sup>24</sup> also observed this incommensurate modulation by electron diffraction, with the same dependence of the wavelength on potassium concentration, but reported that it was induced solely by the electron beam and therefore not a fundamental material property.

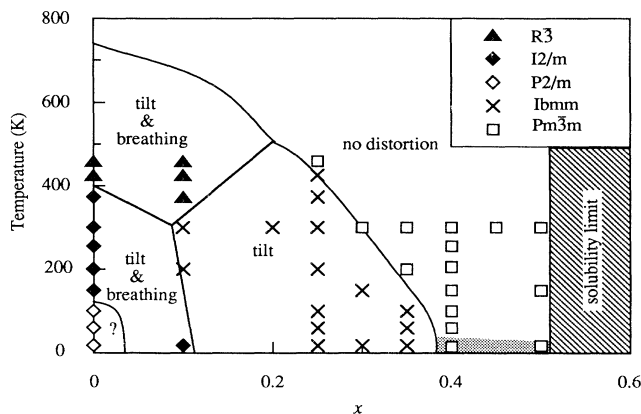


FIG. 1. Phase diagram of  $\text{Ba}_{1-x}\text{K}_x\text{BiO}_3$  as a function of both potassium content ( $x$ ) and temperature [after Pei *et al.* (Ref. 5)]; the particular deformation (breathing mode and/or rigid tilt) of the oxygen framework is indicated. The superconducting phase is schematically represented by the shaded area in the bottom part of the cubic phase.

The interpretation of the modulation has been subject to several speculations. Originally, it was interpreted as an oxygen-vacancy ordering.<sup>22</sup> However, since the modulation wavelength is independent of the oxygen-vacancy concentration over a large range, this interpretation is unlikely. Pei *et al.*<sup>23</sup> interpreted it first as a substitutional type of modulation involving Ba and K atoms, but after additional work,<sup>5</sup> they concluded that it was associated with a charge-density wave that existed for all of the nonsuperconducting compositions (i.e.,  $x < 0.4$ ) regardless of the underlying basic structure. Hewat *et al.*<sup>24</sup> concluded that the modulation could not be interpreted in terms of oxygen-vacancy ordering or K-atom ordering on the Ba sites. They proposed a model involving partial ordering of  $\text{Bi}^{3+}$  versus  $\text{Bi}^{5+}$  atoms accompanied with Bi- or O-atom displacements correlated with the  $\text{Bi}^{3+}$  lone-pair ordering.

In the present work, the structural distortions that give rise to the incommensurate modulation are more fully investigated. Samples of  $\text{Ba}_{1-x}\text{K}_x\text{BiO}_3$  with different potassium content ( $x = 0, 0.2, 0.25, 0.3, 0.35, \text{ and } 0.4$ ) are studied by means of combined electron-diffraction and high-resolution techniques. First, the goal of this investigation was to determine if the modulation is irradiation induced and, if so, to investigate the effect of the electron irradiation on the modulation. Second, the symmetry of the modulation is determined from systematic extinctions in electron-diffraction patterns. The interpretation of these conditions in terms of the superspace formalism allows to derive symmetry-based restrictions on possible modulation models. Third, we will consider the consequences of our findings to the conductivity properties of the material.

### III. OBSERVATIONS

Electron-irradiation experiments have been performed for accelerating voltages ranging from 40 to 400 kV. As long as the accelerating voltage does not exceed 150 kV, it is not expected that even light atoms can be removed from the structure due to electron-atom collisions.<sup>25</sup> On the other hand, oxygen loss (and possibly also loss of potassium<sup>23</sup>) may be caused by local heating of the sample if it is irradiated with a focused electron beam. For ac-

celerating voltages above 200 kV, oxygen loss may be caused due to direct knock-on damage also.

The typical behavior of the investigated  $\text{Ba}_{1-x}\text{K}_x\text{BiO}_3$  samples under electron irradiation is shown in Fig. 2. If precautions are taken in order to minimize the irradiation dose during the orientation of the sample, no satellite reflections are observed [Fig. 2(a)]. Superstructure reflections appear after irradiation, but the irradiation time needed for the satellites to appear varies largely from grain to grain. Figures 2(b) and 2(c) are taken after 10 min and 2 h of irradiation with 100-keV electrons, using a defocused electron beam in order to avoid heating effects. The intensity of the satellite reflections is observed to increase with irradiation time [Figs. 2(b) and 2(c)]. It is important to remark that no qualitative differences in the development of satellite reflections could be detected with respect to irradiation conditions (beam intensity and accelerating voltage).

Around each basic spot, four satellite reflections are observed in  $[001]_p$  zone axis diffraction patterns. The wave vectors that correspond to this modulation can be written as  $\mathbf{q}_1 = (\frac{1}{4} - \epsilon)[110]_p^*$  and  $\mathbf{q}_2 = (\frac{1}{4} - \epsilon)[\bar{1}\bar{1}0]_p^*$ . If the sample is tilted slightly away from this  $[001]_p$  zone axis orientation, one observes that, in total, 12 satellite reflections surround each basic spot and the corresponding wave vectors are parallel with the six  $\langle 110 \rangle_p^*$  directions of the pseudocubic reciprocal lattice. We found that all cubic  $\langle 110 \rangle_p^*$  directions are possible wave-vector orientations, even in the orthorhombic phase; i.e., there is no evidence for correlation between the intrinsic structural distortions of the perovskite structure and the irradiation-induced wave-vector orientation. From high-resolution micrographs, it is observed that the modulated structure is broken up in microdomains of an average size of  $\approx 10$  nm (Fig. 3). In each of these domains, the modulation has a single wave vector. The selected-area electron-diffraction patterns such as in Fig. 2 are interpreted as the superposition of diffraction intensities of different microdomains in the diffracting area. It is thus concluded that the modulation is described by a single wave vector, which can be written as  $\mathbf{q} = (\frac{1}{4} - \epsilon)[110]_p^*$ .

Electron-diffraction patterns of the  $[001]_p$  zone axis orientation of irradiated  $\text{Ba}_{1-x}\text{K}_x\text{BiO}_3$  with different po-

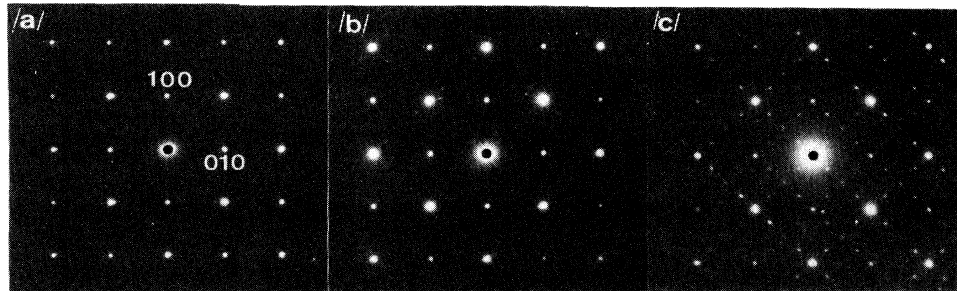


FIG. 2. (a) Electron-irradiation effect observed in a  $[001]_p$  zone axis orientation of  $\text{Ba}_{1-x}\text{K}_x\text{BiO}_3$  ( $x = 0.25$ ) after a few seconds of observation: No satellite reflections are observed. (b) On irradiating the sample with a defocused electron beam, satellite reflections become visible. (c) Their intensity increases and they sharpen up with irradiation dose.

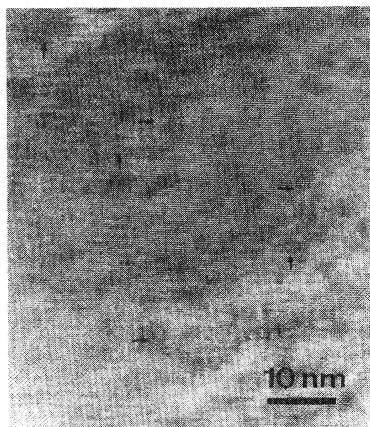


FIG. 3. High-resolution micrograph clearly illustrating the existence of microdomains. In each of these domains, the modulation is single wave vector. The modulation wave vector directions are indicated by small arrows.

tassium concentrations show the systematic variation of the modulation wavelength with the potassium content [Fig. 4(a)]. In Fig. 4(b) the deviation  $\epsilon$  from the commensurate value  $\mathbf{q} = \frac{1}{4}[\mathbf{110}]_p^*$  of the modulation wave vector is plotted as function of the composition. This incommensurability parameter  $\epsilon$  is observed to vary from  $\epsilon = 0.049$  for  $x = 0$  to  $\epsilon = 0$  for  $x = 0.4$ . The presently obtained results agree with the results obtained by Pei *et al.*<sup>23</sup> and Hewat *et al.*<sup>24</sup> for all compounds except for the pure  $\text{BaBiO}_3$  material. In  $\text{BaBiO}_3$  the modulation wave vector, reported previously as  $\mathbf{q} \approx \frac{1}{6}[\mathbf{110}]_p^*$ , is observed after a few minutes of irradiation.

We have also investigated the evolution of the incommensurate modulation with irradiation dose. In contrast with previous reports,<sup>5,23,24</sup> for some of the compositions, a substantial variation of the modulation wavelength is found as a function of the irradiation dose. The results of the irradiation experiments are given in Table I. Rather surprisingly, the change in  $\epsilon$  upon irradiation time was not uniform: Depending on the composition,  $\epsilon$

TABLE I. Variation of the incommensurability parameter  $\epsilon$  with potassium content and irradiation dose. The modulation wave vector is written as  $\mathbf{q} = (\frac{1}{4} - \epsilon)[\mathbf{110}]_p^*$ .  $\epsilon_{\text{begin}}$  is measured at the onset of the modulation, and  $\epsilon_{\text{end}}$  is measured after continued irradiation. Commensurate modulation wave vectors, indicated by an asterisk, are observed for both  $\text{Ba}_{0.6}\text{K}_{0.4}\text{BiO}_3$  and  $\text{BaBiO}_3$ ; in the latter case, a commensurate wave vector  $\mathbf{q} = \frac{1}{6}[\mathbf{110}]_p^*$  is only obtained after longer irradiation.

Sample	$\epsilon_{\text{begin}} (\pm 0.002)$	$\epsilon_{\text{end}} (\pm 0.002)$
$\text{BaBiO}_3$	0.049	0.083*
$\text{Ba}_{0.8}\text{K}_{0.2}\text{BiO}_3$	0.042	0.045
$\text{Ba}_{0.75}\text{K}_{0.25}\text{BiO}_3$	0.025	0.009
$\text{Ba}_{0.7}\text{K}_{0.3}\text{BiO}_3$	0.020	0.020
$\text{Ba}_{0.65}\text{K}_{0.35}\text{BiO}_3$	0.017	0.045
$\text{Ba}_{0.6}\text{K}_{0.4}\text{BiO}_3$	0*	0*

either increased ( $\text{BaBiO}_3$  and  $\text{Ba}_{0.65}\text{K}_{0.35}\text{BiO}_3$ ), decreased ( $\text{Ba}_{0.75}\text{K}_{0.25}\text{BiO}_3$ ) or was left unchanged ( $\text{Ba}_{0.8}\text{K}_{0.2}\text{BiO}_3$ ,  $\text{Ba}_{0.7}\text{BiO}_3$ , and  $\text{Ba}_{0.6}\text{K}_{0.4}\text{BiO}_3$ ). The sample with composition  $\text{Ba}_{0.6}\text{K}_{0.4}\text{BiO}_3$  always showed a commensurate modulation whenever the modulation was detectable.

*In situ* heating of the samples was performed in order to determine if the heating effect plays any role in the formation of the modulation. Contrary to the case of

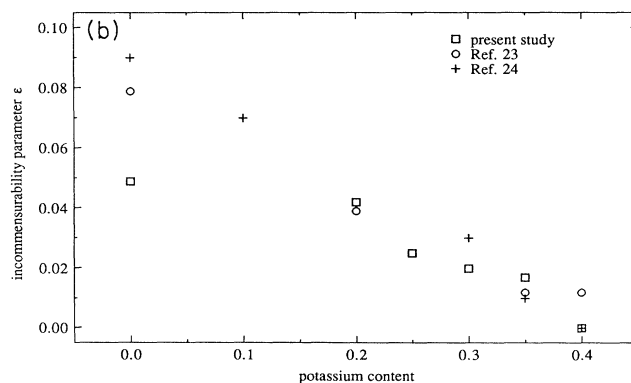
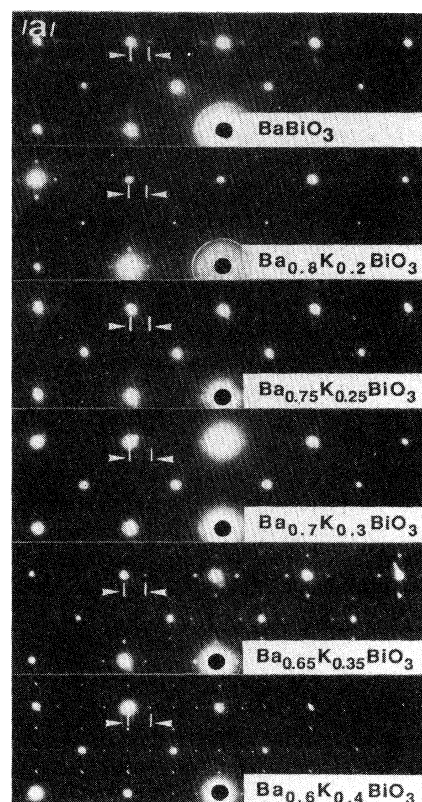


FIG. 4. (a) [001] Electron-diffraction patterns after irradiation showing the variation of the modulation wavelength with potassium content. (b) The incommensurability parameter  $\epsilon$  as measured from electron diffraction patterns. The results are plotted for the case of low irradiation dose. The results reported by Hewat *et al.* (Ref. 24) and Pei *et al.* (Ref. 23) are also represented.

$\text{Nd}_{2-x}\text{Ce}_x\text{CuO}_{4-y}$ , where *in situ* heating facilitates the superlattice formation,<sup>26</sup> it was observed that in  $\text{Ba}_{1-x}\text{K}_x\text{BiO}_3$ , the satellite reflections disappear on heating above 200°C.

The incommensurate satellites which appear after a few minutes of electron irradiation at room temperature disappear after *in situ* heating above 200°C with the electron beam turned off. If the sample is cooled down to room temperature, with the electron beam turned off, the satellite reflections remain extinct. Upon irradiating the same area again, the modulation spots appear again and the cycle may be repeated. It should be noted that the satellite reflections do not disappear if the electron beam is just turned off without heating the sample.

#### IV. INTERPRETATION

Symmetry analysis of incommensurate modulations is worked out in the framework of the superspace formalism developed by De Wolff<sup>27</sup> and De Wolff, Janssen, and Janner.<sup>28</sup> Their method is applied here for the particular case of a single wave-vector modulation in which the wave vector has only one incommensurate component. A superspace symmetry element can be written as  $(R, \epsilon; \mathbf{s}, \delta)$  with  $R$  = point-group symmetry element in three dimensions;  $\epsilon = \pm 1$ , depending on whether or not the incommensurate part of the wave vector is reversed under the operation of  $R$ ;  $\mathbf{s}$  = 3D translational part of the space-group symmetry element;  $\delta$  is the fourth-dimensional translational part of the space-group symmetry element. Considering a symmetry element that transforms a position  $\mathbf{r}_i^0$  in the average structure to a position  $\mathbf{r}_j^0$ , the symmetry condition for a *composition* modulation function  $p(\xi)$  can be written as

$$p_j(\xi) = p_i(\epsilon(\xi - \delta)), \quad (1)$$

with  $\xi = \mathbf{q} \cdot \mathbf{r}_i^0 + \phi$ , where  $\phi$  is an arbitrary phase factor.

Similarly, the condition for a *displacive* modulation function  $\mathbf{u}(\xi)$  is

$$\mathbf{u}_j(\xi) = R \mathbf{u}_i(\epsilon(\xi - \delta)). \quad (2)$$

##### A. Modulation in cubic $\text{Ba}_{1-x}\text{K}_x\text{BiO}_3$ ( $0.3 < x < 0.5$ )

At room temperature and for compositions  $0.3 < x < 0.5$ ,  $\text{Ba}_{1-x}\text{K}_x\text{BiO}_3$  has a simple cubic lattice

with  $Pm\bar{3}m$  space group<sup>5</sup> and unit-cell parameter  $a_p$  ( $\approx 0.43$  nm). If the sample is irradiated, a modulation with wave vector  $\mathbf{q} = (\frac{1}{4} - \epsilon)[110]_p^*$  is induced; the value of  $\epsilon$  ( $0 < \epsilon < 0.045$ ) depends on both the irradiation dose and potassium content. This modulation obviously lowers the point-group symmetry to orthorhombic with Laue group  $mmm$ . This structure will be called the “excubic” phase. The average structure (in the modulated phase) is based on a  $\sqrt{2}a_p \times \sqrt{2}a_p \times a_p$  unit cell. The modulation wave vector  $\mathbf{q}$  is written in the corresponding reciprocal unit cell as  $\mathbf{q} = (\frac{1}{2} - 2\epsilon)[100]^*$ . Reflection conditions are obtained from electron-diffraction tilting experiments (Fig. 5). In this figure indexing of the reflections is performed in the reciprocal unit cell based on the cubic perovskite parameters. The transformation relations between the real-space perovskite base vectors and the actual quasicubic  $\sqrt{2}a_p \times \sqrt{2}a_p \times a_p$  base vectors are

$$\mathbf{a} = \mathbf{a}_p + \mathbf{b}_p, \quad \mathbf{b} = \mathbf{a}_p - \mathbf{b}_p, \quad \mathbf{c} = \mathbf{c}_p.$$

If spots are indexed in the quasicubic reciprocal basis, reflection conditions read as follows:

$$hklm: h + k = 2n, \quad \text{i.e., } C \text{ centering;}$$

$$h0lm: m = 2n, \quad \text{i.e., } \begin{pmatrix} m \\ s \end{pmatrix} (010).$$

Possible superspace groups which conform to these conditions are  $P_{1s1}^{Cmmm}$ ,  $P_{ss1}^{C2mm}$ , and  $P_{1s1}^{Cmm2}$ . From these three the latter two describe structures in which the centrosymmetry is lost due to the modulation. As is expressed by Friedel’s law, it is not possible to detect whether or not the structure is centrosymmetric making use of selected-area diffraction results only. However, a loss of centrosymmetry would give rise to the presence of inversion domains, which can be detected in (real-space) diffraction contrast images (see, e.g. Ref. 29). Such domains have not been found in the present investigation; therefore, the superspace group  $P_{1s1}^{Cmmm}$  is assumed to describe the symmetry of the modulated structure.

The atom positions and superspace site symmetry of the different atom positions in the  $\sqrt{2}a_p \times \sqrt{2}a_p \times a_p$

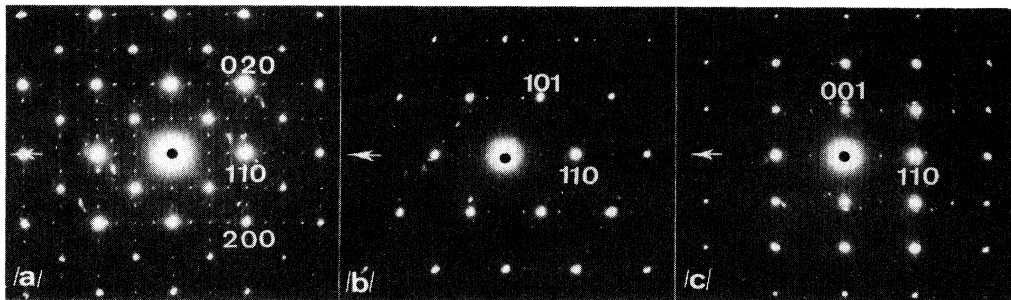


FIG. 5. Tilt experiment (tilt axis is arrowed) on quasicubic  $\text{Ba}_{0.6}\text{K}_{0.4}\text{BiO}_3$  from which the systematic reflection conditions are derived. (a)  $[001]_p$ , (b)  $[111]_p$ , and (c)  $[110]_p$  orientations (indices are based on the perovskite unit cell).

average structure unit cell are listed in Table II. Symmetry restrictions on the modulation function are obtained by applying the superspace site symmetry elements to a composition or to a displacive modulation (for more details on the method, see Ref. 30). Symmetry restrictions are worked out entirely for a composition modulation  $p(\xi)$ . The restrictions on Ba or K, Bi, and O(1) atoms are the same and are given by

$$p^{(1)}(\xi) = p^{(1)}(-\xi) \begin{bmatrix} m_x \\ 1 \end{bmatrix} \quad (3a)$$

$$= p^{(1)}(\xi - \frac{1}{2}) \begin{bmatrix} m_y \\ s \end{bmatrix} \quad (3b)$$

$$= p^{(1)}(\xi) \begin{bmatrix} m_z \\ 1 \end{bmatrix}. \quad (3c)$$

From the Fourier expansion of the modulation function, only the first Fourier term is taken into account since refinement of the shape of the modulation wave is virtually impossible using electron-diffraction techniques only. The occupation modulation function is written as

$$p(\xi) = \alpha_1 \exp(2\pi i \xi) + \alpha_{\bar{1}} \exp(-2\pi i \xi). \quad (4)$$

Substitution of conditions (3a) and (3b) in expression (4) gives

$$\alpha_1^{(1)} = \alpha_{\bar{1}}^{(1)} \quad [\text{from (3a)}],$$

$$\alpha_1^{(1)} = -\alpha_{\bar{1}}^{(1)} \quad [\text{from (3b)}]$$

and, therefore,

$$\alpha_1^{(1)} = \alpha_{\bar{1}}^{(1)} = 0. \quad (5)$$

The symmetry conditions on O(2) atoms are given by

$$p^{(2)}(\xi) = p^{(2)}(-\xi + \frac{1}{2}) \begin{bmatrix} 2_z \\ s \end{bmatrix} \quad (6a)$$

$$= p^{(2)}(\xi) \begin{bmatrix} m_z \\ 1 \end{bmatrix}. \quad (6b)$$

TABLE II. Inequivalent average atom positions in the quasicubic  $\sqrt{2}a_p \times \sqrt{2}a_p \times a_p$  unit cell. The special positions in this unit cell are denoted by the standard symbols of the International Tables. The last column contains the superspace site symmetry in the notation of De Wolf, Janssen, and Janner (Ref. 28) of the different atoms in irradiated quasicubic  $\text{Ba}_{1-x}\text{K}_x\text{BiO}_3$ .

Atom type	$x$	$y$	$z$	Superspace site symmetry
Ba,K (2a)	0	0	0	$mmm$ $\frac{1}{s} s s$
Bi (2b)	$\frac{1}{2}$	0	$\frac{1}{2}$	$mmm$ $\frac{1}{s} s s$
O(1) (2c)	$\frac{1}{2}$	0	0	$mmm$ $\frac{1}{s} s s$
O(2) (4f)	$\frac{1}{4}$	$\frac{1}{4}$	$\frac{1}{2}$	$2/m$ $\frac{s}{s} 1$

Substituting (6a) in (4), one gets

$$\alpha_1^{(2)} = -\alpha_{\bar{1}}^{(2)}. \quad (7)$$

Starting from Eq. (2) and following the same procedure, the conditions for a displacive modulation are obtained. The results for both kinds of modulation are given in Table III.

### B. Modulation in orthorhombic $\text{Ba}_{1-x}\text{K}_x\text{BiO}_3$ ( $0.1 < x < 0.3$ )

As-grown  $\text{Ba}_{1-x}\text{K}_x\text{BiO}_3$  with  $0.1 < x < 0.3$  is orthorhombic at room temperature. It has  $Ibmm$  space-group symmetry and is based on a  $\sqrt{2}a_p \times \sqrt{2}a_p \times 2a_p$  unit cell. On irradiating, the same type of satellite reflections are observed as in quasicubic  $\text{Ba}_{1-x}\text{K}_x\text{BiO}_3$  ( $x > 0.3$ ). From tilting experiments (see Fig. 6), one observes around each pseudocubic basic reflection 12 satellite reflections (as is also the case for quasicubic  $\text{Ba}_{1-x}\text{K}_x\text{BiO}_3$ ). High-resolution micrographs show that the modulated structure consists of a patchwork of microdomains. Within each microdomain the modulation is single wave vector, and in each of the orthorhombic orientation variants, which result from a tilt of the octahedra, irradiation-induced microdomains with wave-vector orientation along all formerly equivalent  $\langle 110 \rangle_p^*$  directions are observed. These  $\langle 110 \rangle_p^*$  directions are noncrystallographic directions in the orthorhombic unit cell. The symmetry is thus lowered to triclinic, and few symmetry-based restrictions on the modulation function are to be expected.

With this in mind, a complete description of the modulation in four-dimensional space based on an average triclinic structure is not performed, but the extinction conditions are interpreted in the orthorhombic reciprocal basis. The transformation relations between the real-space perovskite base vectors and the orthorhombic  $\sqrt{2}a_p \times \sqrt{2}a_p \times 2a_p$  base vectors are

$$\mathbf{a} = \mathbf{a}_p + \mathbf{b}_p, \quad \mathbf{b} = \mathbf{a}_p - \mathbf{b}_p, \quad \mathbf{c} = 2\mathbf{c}_p.$$

Electron-diffraction tilting experiments (Fig. 6) allow one to determine reflection conditions. If spots are indexed in the reciprocal unit cell based on the  $\sqrt{2}a_p \times \sqrt{2}a_p \times 2a_p$  base vectors, reflection conditions read as follows:

$$hklm: h + k + l = 2n, \quad \text{i.e., } I \text{ centering};$$

$$hklm: h + k = 2n \quad (\text{or } l = 2n), \quad \text{for } m \neq 0;$$

$$oklm: k = 2n, \quad \text{i.e., } b(100);$$

TABLE III. Symmetry restrictions on the first Fourier term of a composition or displacive modulation. The restriction on Ba, Bi, and O(1) sites is identical since they have the same superspace site symmetry.

	$u_x(\xi)$	$u_y(\xi)$	$u_z(\xi)$	$p(\xi)$
Ba(K),BiO(1)	0	$\cos(2\pi\xi)$	0	0
O(2)	$\cos(2\pi\xi)$	$\cos(2\pi\xi)$	0	$\sin(2\pi\xi)$

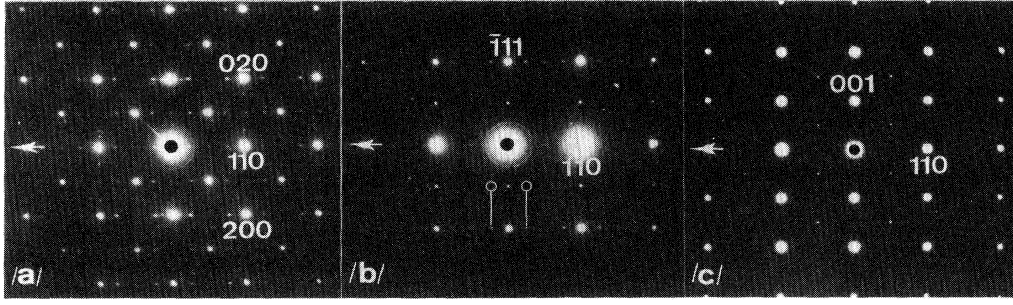


FIG. 6. Tilt experiment (tilt axis arrowed) on quasiorthorhombic  $\text{Ba}_{0.8}\text{K}_{0.2}\text{BiO}_3$  from which the systematic reflection conditions are derived. (a)  $[001]_p$ , (b)  $[\bar{1}1\bar{2}]_p$ , and (c)  $[1\bar{1}0]_p$  orientation (indices are based on the perovskite unit cell). Small open circles indicate the absence of satellite reflections around  $(hkl)_p, l = n + \frac{1}{2}$  spots.

$$h0lm: m=2n, \text{ i.e., } \begin{pmatrix} m \\ s \end{pmatrix} (010).$$

The condition  $h+k=2n$  (or  $l=2n$ ) that holds for satellite reflections, cannot be written as a superspace Bravais lattice condition. Such a condition corresponds to a  $C$ -centering condition in normal 3D space, which holds for satellite reflections only. Extinctions of satellite reflections obeying this condition are expected if the modulation involves only atoms situated at special positions (Wyckoff positions) in the unit cell which conform to  $C$  centering (apart from the body centering of the Bravais lattice) and if the modulation does not break this symmetry. In the basic structure of orthorhombic  $\text{Ba}_{1-x}\text{K}_x\text{BiO}_3$ , only the bismuth atoms are positioned on  $C$ -centered sites (Table IV) and are therefore the only ones responsible for the modulation.

The absence of satellite reflections around the  $l$ -odd basic structure reflections can also be understood intuitively. These reflections ( $l$ -odd,  $m=0$ ) result from the rigid tilt distortions of the octahedra framework. If the incommensurate modulation involves only atoms of which the position is left unchanged by the octahedral tilt, one does not expect to observe satellite reflections around these  $l$ -odd basic reflections. At the same time, this explains the absence of a correlation of the modulation-induced microdomains and the basic structure orthorhombic domains.

TABLE IV. Atom positions for  $\text{Ba}_{0.8}\text{K}_{0.2}\text{BiO}_3$  at 295 K. The unit-cell parameters are  $a=0.61280$  nm,  $b=0.61040$  nm, and  $c=0.86286$  nm, and the structure has orthorhombic  $Ibmm$  space group. In the last column, reflection conditions resulting from special positions are given.

	$x$	$y$	$z$	Special conditions
Ba,K (4e)	0.507	0	$\frac{1}{4}$	none
Bi (4a)	0	0	0	$hkl: l=2n$
O(1) (4e)	0.047	0	$\frac{1}{4}$	none
O(2) (8g)	$\frac{1}{4}$	$\frac{1}{4}$	0.9884	$hkl: k=2n$

## V. COMBINATION OF THE RESULTS AND PROPOSITION OF A MODEL

If it is logically assumed that the modulation is of the same type for all compositions, we can combine the restrictions obtained from diffraction results on orthorhombic and cubic  $\text{Ba}_{1-x}\text{K}_x\text{BiO}_3$ . From the diffraction on orthorhombic  $\text{Ba}_{1-x}\text{K}_x\text{BiO}_3$ , it is concluded that only bismuth atoms are involved in the modulation, and from Table III, it is read that bismuth atoms can only be *displacively* modulated. The final modulation model is represented in the  $\sqrt{2}a_p \times \sqrt{2}a_p \times a_p$  unit cell: It is a transverse displacive wave with wave vector parallel to the  $x$  axis and displacements parallel to the  $y$  axis. The phase relationship between the two Bi atoms in the  $\sqrt{2}a_p \times \sqrt{2}a_p \times a_p$  unit cell can also be obtained from relation (2).

The symmetry relationship that connects the two equivalent Bi positions in this unit cell is a twofold axis parallel with the  $z$  axis. In the superspace group, this symmetry operation becomes  $(\frac{1}{2})$ , i.e.,  $\epsilon = -1$  and  $\delta = \frac{1}{2}$ . Substitution in (2) yields, for the displacements along the  $y$  direction,

$$u_2^y(\xi) = -u_1^y(-\xi + \frac{1}{2}). \quad (8)$$

This leads to the following relation between the displacement of the two inequivalent bismuth positions:

$$\begin{aligned} A_2^y \cos 2\pi\xi &= -A_1^y \cos[2\pi(-\xi + \frac{1}{2})] \\ &= A_1^y \cos 2\pi\xi \end{aligned}$$

or

$$A_2^y = A_1^y. \quad (9)$$

The variable  $\xi$  is determined upon a constant term  $\phi$ , which controls the actual phase of the modulation function. In the case of an incommensurate modulation,  $\phi$  is not determined. For the commensurate modulation in  $\text{Ba}_{0.6}\text{K}_{0.4}\text{BiO}_3$ , the value  $\frac{1}{8}$  is attributed to  $\phi$  in order to explain the displacements observed in the high-resolution image (Fig. 7). In this image, observed under grazing an-

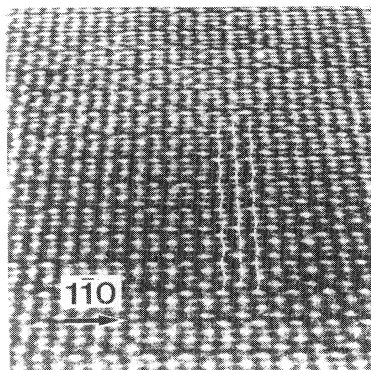


FIG. 7. High-resolution micrograph viewed under grazing angle, showing the displacive modulation of the brighter dots.

gle, one can detect the displacements of the brightest dots, as indicated by the dashed lines. A schematic representation for the modulation is given in Fig. 8. Displacement amplitudes can be estimated from the high-resolution image as  $\approx 0.005$  nm.

## VI. DISCUSSION

From the symmetry considerations presented in the above paragraph, it is concluded that the modulation involves only a displacement of the bismuth atoms. On this basis the models that invoke a chemical ordering of the barium and potassium atoms and those which assume an ordering of oxygen vacancies can be excluded. The interpretation of the modulation as an ordering of  $\text{Bi}^{3+}$ - $\text{Bi}^{5+}$  is also ruled out since the displacements of the bismuth atoms are too small to result in a complete charge disproportionation. On the basis of the present electron microscopy investigations, it is concluded that partial charge disproportionation due to bismuth displacements in a rigid oxygen octahedra framework occurs. The

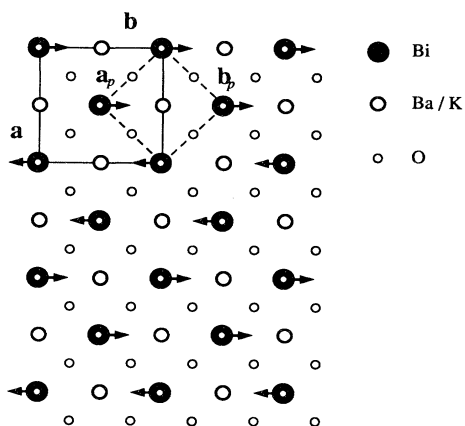


FIG. 8. Schematic drawing of the modulation in  $\text{Ba}_{1-x}\text{K}_x\text{BiO}_3$  represented a projection of the structure along the  $[001]$  direction. Bi atoms are represented as solid circles, Ba or K atoms as large open circles, and oxygen atoms as small open circles.

structure investigations, however, do not give clues on the driving force behind the modulation.

In view of the fact that the incommensurate satellite reflections are only observed after electron irradiation (Fig. 2), it might be concluded that the modulation is irradiation induced, e.g., as an oxygen vacancy induced effect, and that it is not a fundamental material property. This, however, is very difficult to accept in view of the very low threshold accelerating voltage (below 40 kV). Elementary collision theory shows that the maximum energy transmitted to oxygen atoms from 40-keV electrons is  $\approx 5$  eV. This energy is far too low for the creation of oxygen vacancies. A model which is consistent with our results is that of a time-fluctuating partial charge disproportionation of the bismuth atoms due to displacement from their average positions. Upon irradiating the material with electrons, it is possible to induce clustering of *already existing* point defects (such as, e.g., oxygen vacancies), even at very low energy transfers. Such clusters of point defects can then act as pinning centers for the modulation. A disordering of the pinning centers may then account for the disappearance of the satellite reflections on heating above 200 °C.

The gradual increase in satellite reflection intensity can be understood as an alignment effect: The energy transfer of  $\approx 0.4$  eV to bismuth atoms by 40-keV electrons is far too low to cause knock-on damage, but it is high enough to cause atom vibrations and thus to overcome potential barriers between a state in which two neighboring bismuth sites are modulated in two different directions and a state in which these sites are modulated with the same wave vector. Dynamic electron microscopy observations show sometimes a change in the modulation wave vector within one microdomain from one direction to another. The assumed growth of microdomains also reduces domain-boundary effects and explains both the variation of the modulation wavelength and the sharpening of the satellite reflections with electron-irradiation dose.

This structural modulation of the bismuth atoms can account for the conductivity properties of  $\text{Ba}_{1-x}\text{K}_x\text{BiO}_3$ . As long as the modulation is incommensurate with the underlying lattice periodicity, the bismuth atom displacements are not equal over the whole sample. Making use of simple valence summation rules, one obtains a varying valence of the bismuth atoms; i.e., one has charge disproportionation which can explain the semiconducting behavior in this composition range. On the other hand, the model obtained on basis of electron-diffraction and high-resolution methods for the commensurate modulation in  $\text{Ba}_{0.6}\text{K}_{0.4}\text{BiO}_3$  shows displacements of the bismuth atoms which are equal in magnitude for all bismuth atoms. Therefore, no charge disproportionation is evidenced in this case, and metallic behavior is expected.

## ACKNOWLEDGMENTS

Various stimulating discussions with Professor J. Van Landuyt and Professor S. Amelinckx are gratefully acknowledged. This work has been performed in the framework of the Institute for Materials Science (IMS) of the

University of Antwerp under an IUAP contract with the Ministry of Science Policy. At Argonne, this work was supported by the U. S. Department of Energy, Division of Basic Energy Sciences—Materials Sciences, under Contract No. W-31-109-ENG-38 (D.G.H., D.R.R., A.W.M.,

and J.D.J.), and the National Science Foundation, Science and Technology Center for Superconductivity, under Grant No. DMR-88-09854 (D.T.M. and S.P.). M. V. received support from the National Fund for Scientific Research (Belgium).

- <sup>1</sup>J. G. Bednorz and K. A. Müller, *Z. Phys. B* **64**, 189 (1986).
- <sup>2</sup>A. W. Sleight, J. L. Gillson, and P. E. Bierstedt, *Solid State Commun.* **17**, 27 (1975).
- <sup>3</sup>L. F. Mattheiss, E. M. Gyorgy, and D. W. Johnson, Jr., *Phys. Rev. B* **37**, 3745 (1988).
- <sup>4</sup>R. J. Cava, B. Batlogg, J. J. Krajewski, R. Farrow, L. W. Rupp, Jr., A. E. White, K. Short, W. F. Peck, and T. Kometani, *Nature* **332**, 814 (1988).
- <sup>5</sup>S. Pei, J. D. Jorgensen, B. Dabrowski, D. G. Hinks, D. R. Richards, A. W. Mitchell, J. M. Newsam, S. K. Sinha, D. Vaknin, and A. J. Jacobson, *Phys. Rev. B* **41**, 4126 (1990).
- <sup>6</sup>D. E. Cox, and A. W. Sleight, *Solid State Commun.* **19**, 969 (1976).
- <sup>7</sup>D. E. Cox, and A. W. Sleight, *Acta Crystallogr. B* **35**, 1 (1979).
- <sup>8</sup>G. Thornton and A. J. Jacobson, *Acta Crystallogr. B* **34**, 351 (1978).
- <sup>9</sup>C. Chaillout, J. P. Remeika, A. Santoro, and M. Marezio, *Solid State Commun.* **56**, 829 (1985).
- <sup>10</sup>C. Chaillout, A. Santoro, J. P. Remeika, A. S. Cooper, G. P. Espinosa, and M. Marezio, *Solid State Commun.* **65**, 1363 (1988).
- <sup>11</sup>A. M. Glazer, *Acta Crystallogr. B* **28**, 3384 (1972).
- <sup>12</sup>L. F. Mattheiss, and D. R. Hamann, *Phys. Rev. B* **28**, 4227 (1983).
- <sup>13</sup>T. Nakamura, K. Saburo, and T. Sata, *J. Phys. Soc. Jpn.* **31**, 1284 (1971).
- <sup>14</sup>D. G. Hinks, B. Dabrowski, J. D. Jorgensen, A. W. Mitchell, D. R. Richards, S. Pei, D. Shi, and *Nature* **333**, 836 (1988).
- <sup>15</sup>B. Dabrowski, D. G. Hinks, J. D. Jorgensen, R. K. Kalia, P. Vashishta, D. R. Richards, D. T. Marx, and A. W. Mitchell, *Physica C* **156**, 24 (1988).
- <sup>16</sup>H. Sato, S. Tajima, H. Takagi, and S. Uchida, *Nature* **338**, 241 (1989).
- <sup>17</sup>C. Methfessel and S. Methfessel, in *Superconductivity in d- and f-Band Metals*, edited by W. Buckel and W. Weber (Kernforschungszentrum, Karlsruhe, 1982), p. 393.
- <sup>18</sup>T. M. Rice and L. Sneddon, *Phys. Rev. Lett.* **47**, 689 (1981).
- <sup>19</sup>E. Jurczek and T. M. Rice, *Europhys. Lett.* **1**, 225 (1986).
- <sup>20</sup>W. Weber, *Jpn. J. Appl. Phys.* **26**, Suppl. 3, 981 (1987).
- <sup>21</sup>C. M. Varma, *Phys. Rev. Lett.* **61**, 2713 (1988).
- <sup>22</sup>C. Chaillout and J. P. Remeika, *Solid State Commun.* **56**, 833 (1985).
- <sup>23</sup>S. Pei, N. J. Zaluzec, J. D. Jorgensen, B. Dabrowski, D. G. Hinks, A. W. Mitchell, and D. R. Richards, *Phys. Rev. B* **39**, 811 (1989).
- <sup>24</sup>E. A. Hewat, C. Chaillout, M. Godinho, M. F. Gorius, and M. Marezio, *Physica C* **157**, 228 (1989).
- <sup>25</sup>D. G. Howitt, in *Principles of Analytical Electron Microscopy*, edited by D. C. Joy, A. D. Romig, Jr., and J. I. Goldstein (Plenum, New York, 1986), p. 375.
- <sup>26</sup>C. H. Chen, D. J. Werder, A. C. W. P. James, D. W. Murphy, S. Zahurak, R. M. Fleming, B. Batlogg, and L. F. Schneemeyer, *Physica C* **160**, 375 (1988).
- <sup>27</sup>P. M. De Wolff, *Acta Crystallogr. A* **33**, 493 (1977).
- <sup>28</sup>P. M. De Wolff, T. Janssen, and A. Janner, *Acta Crystallogr. A* **37**, 625 (1981).
- <sup>29</sup>S. Amelinckx and J. Van Landuyt, in *Diffraction and Imaging Techniques in Material Science*, edited by S. Amelinckx, R. Gevers, and J. Van Landuyt (North-Holland, Amsterdam, 1978), p. 107.
- <sup>30</sup>M. Verwerft and G. Van Tendeloo, *J. Electron Microsc. Technol.* **17**, 70 (1991).

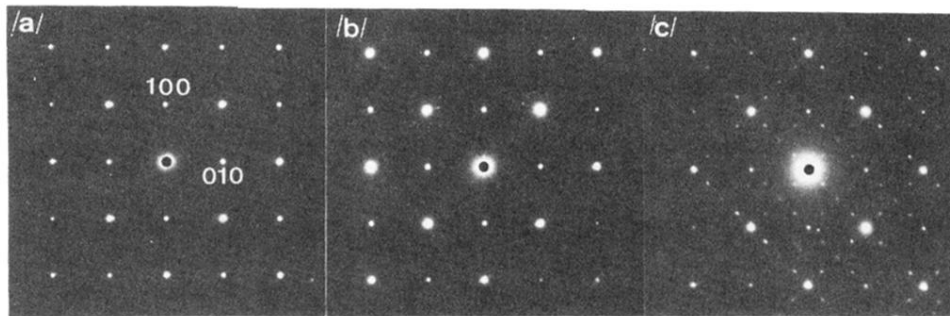


FIG. 2. (a) Electron-irradiation effect observed in a [001] zone axis orientation of  $\text{Ba}_{1-x}\text{K}_x\text{BiO}_3$  ( $x=0.25$ ) after a few seconds of observation: No satellite reflections are observed. (b) On irradiating the sample with a defocused electron beam, satellite reflections become visible. (c) Their intensity increases and they sharpen up with irradiation dose.

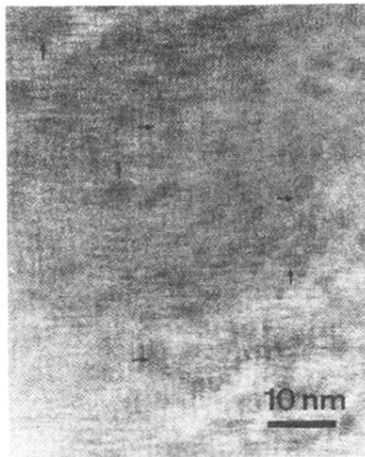


FIG. 3. High-resolution micrograph clearly illustrating the existence of microdomains. In each of these domains, the modulation is single wave vector. The modulation wave vector directions are indicated by small arrows.

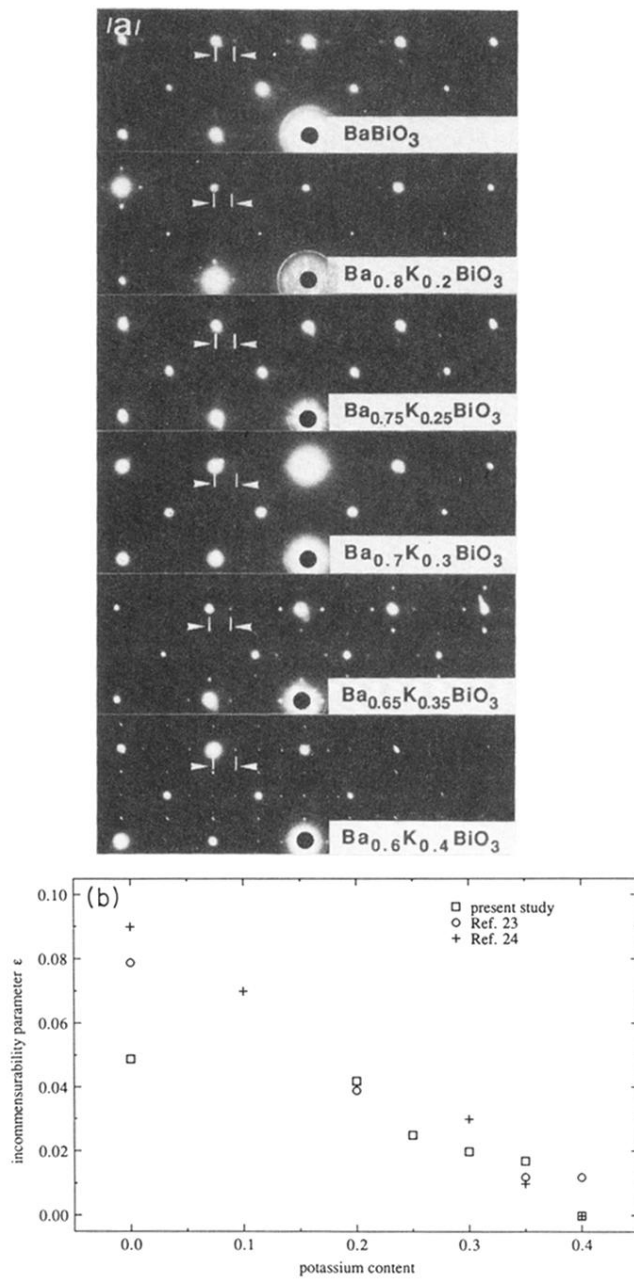


FIG. 4. (a) [001] Electron-diffraction patterns after irradiation showing the variation of the modulation wavelength with potassium content. (b) The incommensurability parameter  $\epsilon$  as measured from electron diffraction patterns. The results are plotted for the case of low irradiation dose. The results reported by Hewat *et al.* (Ref. 24) and Pei *et al.* (Ref. 23) are also represented.

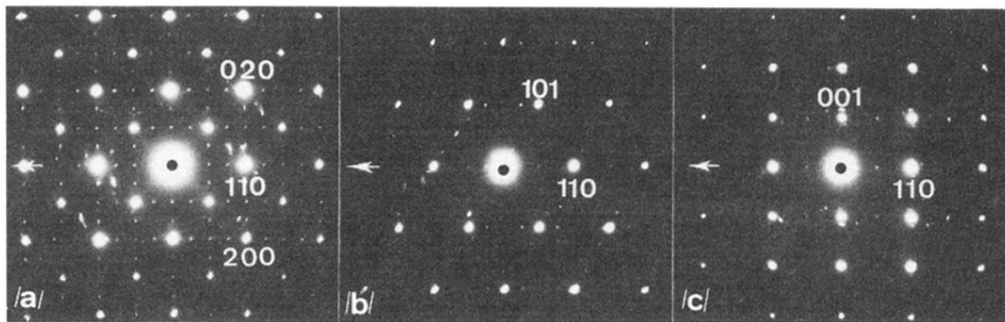


FIG. 5. Tilt experiment (tilt axis is arrowed) on quasicubic  $\text{Ba}_{0.6}\text{K}_{0.4}\text{BiO}_3$  from which the systematic reflection conditions are derived. (a)  $[001]_p$ , (b)  $[\bar{1}\bar{1}\bar{1}]_p$ , and (c)  $[\bar{1}\bar{1}0]_p$  orientations (indices are based on the perovskite unit cell).

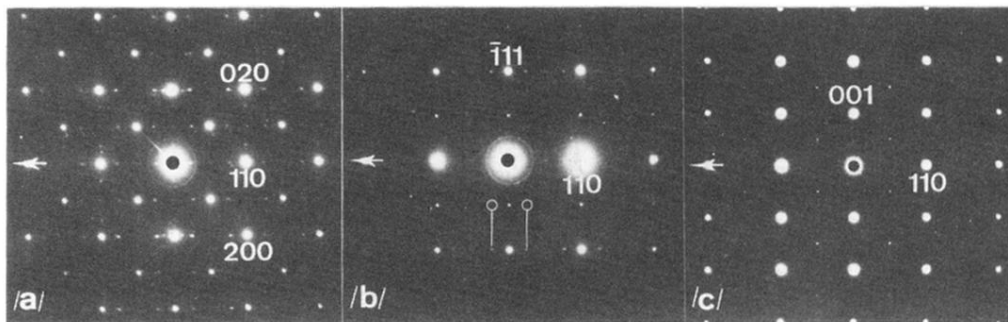


FIG. 6. Tilt experiment (tilt axis arrowed) on quasiorthorhombic  $\text{Ba}_{0.8}\text{K}_{0.2}\text{BiO}_3$  from which the systematic reflection conditions are derived. (a)  $[001]_p$ , (b)  $[\bar{1}\bar{1}\bar{2}]_p$ , and (c)  $[1\bar{1}0]_p$  orientation (indices are based on the perovskite unit cell). Small open circles indicate the absence of satellite reflections around  $(hkl)_p l = n + \frac{1}{2}$  spots.

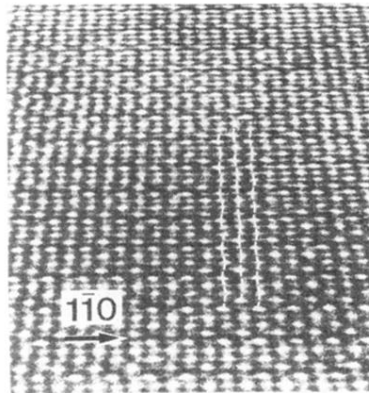


FIG. 7. High-resolution micrograph viewed under grazing angle, showing the displacive modulation of the brighter dots.